Studies of N = Z nuclei beyond ^{56}Ni

D. Rudolph

7. Studies of *N*~*Z* nuclei beyond ^{56}Ni*

7.1. Introduction

The study of nuclei far from stability at the extreme values of *N/Z* is one of the major incentives of the existing and projected radioactive ion-beam facilities around the world. By investigating such exotic species certain terms of the nuclear Hamiltonian can be viewed under a magnifying glass, which are otherwise difficult to access. The region of interest of the nuclidic chart, namely *N*~*Z* nuclei between ^{40}Ca and ^{100}Sn is shown in Figure 7.1 together with some of the physics issues that have been addressed by EUROBALL studies. The horizontal and vertical lines in this figure mark the magic and semi-magic numbers 20, 28, 40, and 50, and the red squares represent the compound nuclei formed in the fusion-evaporation reactions used in the experiments. The size of these squares scales with the number of experiments, i.e., the larger the square the more studies employed a given compound nucleus.

In a typical fusion-evaporation experiment aimed at the spectroscopy of *N*~*Z* nuclei, 20 to 30 different residual nuclei are populated with relative cross sections ranging from fractions of a percent up to more than 30%. Since the nuclei of interest are often those with tiny cross-sections, involving one or even multiple neutron evaporation, the coincident detection of γ rays and evaporated neutrons is of vital importance. Despite their significant contribution to the aspect of reaction channel selection, the charged-particle detection arrays surrounding the target serve yet another issue. The exclusive measurement of energies and momenta of the evaporated neutrons, protons, and especially α-particles has enabled an event-by-event determination of the velocity vector of the recoiling nuclei. Depending on the mass region and the nucleus of interest, this kinematical correction procedure may improve the γ-ray energy

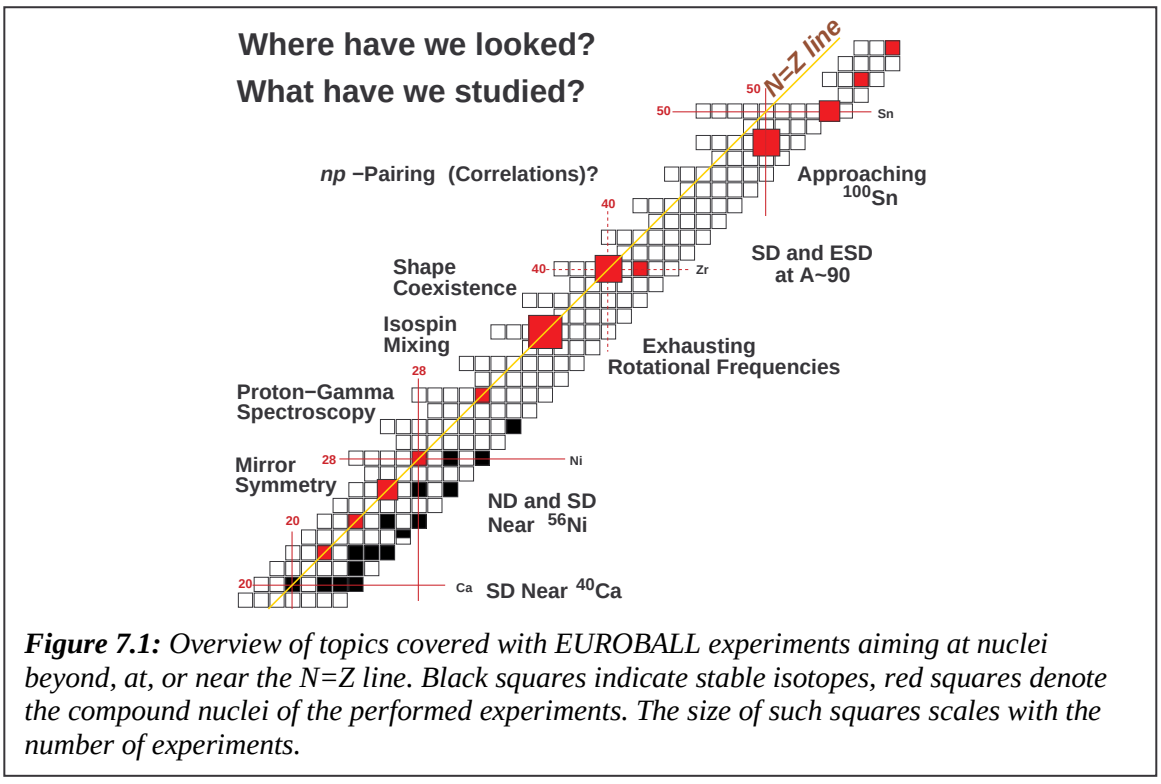

Figure 7.1: *Overview of topics covered with EUROBALL experiments aiming at nuclei beyond, at, or near the N=Z line. Black squares indicate stable isotopes, red squares denote the compound nuclei of the performed experiments. The size of such squares scales with the number of experiments.*

* Contribution by D. Rudolph

resolution by a factor of two to three, which in turn increases the sensitivity of the experimental set-up by almost the same magnitude.

It is important to note that up to ^{40}Ca the line of stability coincides with the N=Z line, which is marked by the yellow diagonal line in Figure 7.1. Beyond ^{56}Ni, however, the line of stability bends more and more towards more neutron-rich nuclei, such that ^{100}Sn is twelve neutrons away from the most neutron-deficient, stable Sn isotope ^{112}Sn. ^{100}Sn is the last particle bound N=Z nucleus, while the proton drip line more or less equals the N=Z line starting from mass A~70 for the odd-Z nuclei.

Medium heavy nuclei on the neutron deficient side of the valley of stability can be produced using a combination of stable beams and targets. But the increasing difference between the stable isotopes and the N=Z line puts severe constraints on the present-day experimental possibilities: ^{80}Zr marks the heaviest N=Z compound nucleus, which can be formed with stable beams and targets, namely via the reaction ^{40}Ca+^{40}Ca. This implies that up to ^{72}Kr even-even N=Z nuclei can be studied via 2α-evaporation. Starting from ^{76}Sr and up to ^{96}Cd the possible reaction channels involve two-neutron evaporation, while the population of excited states in ^{100}Sn would imply the evaporation of four neutrons. This scheme is reflected by the compound nuclei chosen for the EUROBALL experiments (cf. red squares in Figure 7.1). Similarly, odd-odd N=Z nuclei up to ^{78}Y can be reached via 1p1n- or 1α1p1n reactions, while the study of heavier odd-odd N=Z nuclei requires the population via three neutron evaporation.

It is important to recall that the evaporation of any additional neutron typically reduces the relative cross section by a factor of fifty to hundred, on top of the general decrease of the cross section with increasing mass, i.e., ~2 mb for ^{56}Ni down to ~1 μb in the case of ^{96}Cd. In-beam studies with present-day techniques and available stable beam-target combinations can probe cross section down into the few μb regime. However, it is not only the absolute but also the relative cross section which is of importance. Depending on the efficiency and quality of the channel selection, tiny components (< 0.1%) of heavier, more neutron-rich isotopes of the target species or common problems with oxygen and/or carbon contaminations of the target material may inhibit a clear identification of exotic reaction channels. It appears that studies of N=Z nuclei beyond ^{96}Cd and ^{78}Y, respectively, have to await more efficient future spectrometers in conjunction with intense radioactive beams.

7.2. Exotic decays

For nuclei above mass A = *40* the N = Z line drifts more and more away from the line of stability with increasing mass of the nuclei. Together with a rather small Coulomb barrier this gives rise to an intriguing facet of the heavier N ~ Z nuclei, namely that proton, α-, or even cluster emission may play a role in the decay of their excited states. For a more general recent review of in-beam and decay work of N~Z nuclei we refer to [177]. Another related facet of medium-mass N~Z nuclei is the astrophysical rapid proton capture process, which is thought to follow them from about mass A~60 up to ^{100}Sn. A number of nuclear structure features of specific N=Z nuclei provide important input into the respective modelling of stellar evolution scenarios (see, e.g., Ref. [178]).

Soon after the mass A ~ 60 regime had been marked as a region of superdeformed nuclear shapes [179], some of the rotational bands associated with the second minimum of the nuclear

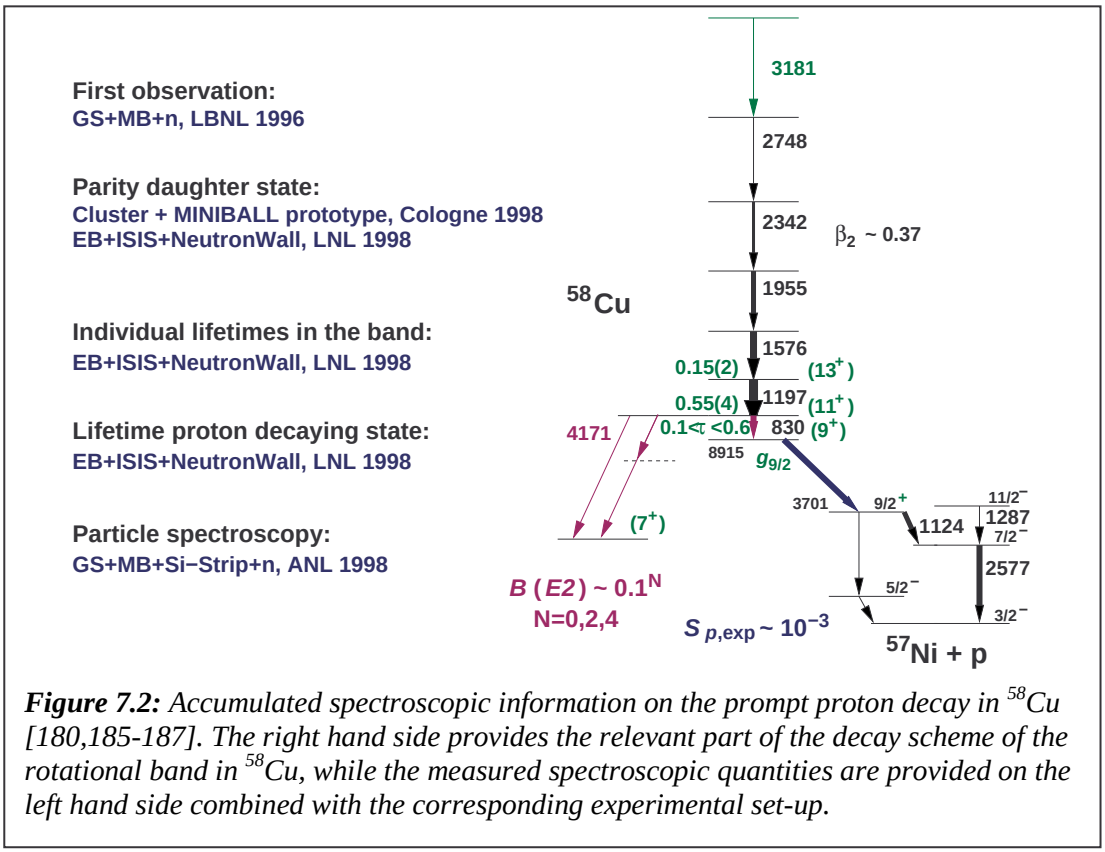

Figure 7.2: *Accumulated spectroscopic information on the prompt proton decay in ^{58}Cu [180,185-187]. The right hand side provides the relevant part of the decay scheme of the rotational band in ^{58}Cu, while the measured spectroscopic quantities are provided on the left hand side combined with the corresponding experimental set-up.*

potential were found to decay via mono-energetic prompt proton- or α-particle emission [180-184]. This new particle decay mode, which was first established in ^{58}Cu [180] competes with in-band and γ-ray linking transitions between the well- (or super-) deformed states and the spherical states in the first minimum of the potential energy surface. In ^{58}Cu the prompt proton decay connects the lowest observed state in the rotational band with the spherical neutron $g_{9/2}$ single-particle state in ^{57}Ni [185].

The relevant part of the decay scheme of ^{58}Cu is provided in Figure 7.2. The left hand side of Figure 7.2 describes the progress in terms of spectroscopic information regarding the ^{58}Cu case starting from the first observation of the new decay in 1998 [180] until 2002. Within this period, the spin and parity of the daughter state in ^{57}Ni was determined [185], spins and parities were tentatively assigned to the band members, lifetimes of the low lying states in the band were measured [111], and last but not least the lifetime of the proton-decaying state could be limited to 0.1 ps < τ < 0.6 ps [186].

The latter two results were obtained from an experiment performed with EUROBALL coupled to the 4π ΔE-E Si-array ISIS [2] and the Neutron Wall [5]. The use of a backed target allows the Doppler Shift Attenuation Method (DSAM) to be used to determine lifetimes. The 830 keV line, which depopulates the 9745 keV state and feeds the proton-decaying level at 8915 keV, reveals both a stopped and a shifted component in its lineshape observed in the backward-angle Cluster section of EUROBALL. Therefore, energy correlations between the 830 keV γ ray measured in the Cluster detectors and the 2.3 MeV proton peak in the most forward detector elements of ISIS have been studied successfully, and it was possible to derive the above mentioned lifetime limits for the proton decaying state [186]. This experiment was the first attempt to perform in-beam high-resolution particle-γ coincidence spectroscopy.

Lifetime measurements of the γ- and proton-decaying states suggest a similar hindrance for the single-step 4171 keV γ-ray transition and the $g_{9/2}$ proton decay. In fact, the proton decay appears to be somewhat less hindered (~10^{-3}) than the single-step γ decay (~10^{-4}). One possible explanation is that the emission of the $g_{9/2}$ proton naturally helps in reducing the deformation of the system, because it is moving in the shape driving orbit located more towards the surface of the deformed ^{58}Cu nucleus. It is also interesting to note that the deformation of the rotational band in ^{58}Cu increases towards the bottom of the band - more than expected employing contemporary mean-field calculations [111]. Similar to ^{60}Zn [188], there is evidence in ^{58}Cu that the decay-out from the second minimum in $N = Z$ nuclei in the mass $A \sim 60$ region is rather selective - a scenario which is supported by the suppression of isoscalar dipole transitions in such nuclei, the low level density, and the small number of particles which need to be rearranged in the decay process.

7.3. The mass $A \sim 70$ - 80 region

One possible indicator for the enhancement of neutron-proton pair correlations in $N = Z$ nuclei is a delay of the alignment frequency of high-j orbits. In the mass $A \sim 70$ - 80 region all even-even $N = Z$ nuclei between ^{72}Kr and ^{88}Ru exhibit such a delay of alignment of $g_{9/2}$ particles with respect to rotational bands in odd-A and $N = Z + 2$ even-even neighbours [189-192]. However, this mass region is also well known for sudden and drastic shape changes as a function of nucleon number and excitation energy, which clearly affect the band crossing phenomena. Therefore, it is equally important to study the nearest neighbours and check carefully, whether or not their structure can be explained with nuclear structure models that do not specifically include neutron-proton pair correlations. If the same models subsequently fail to reproduce the excitation pattern of the $N = Z$ nuclei, then the presence of such pairing modes could be evidenced.

On the left hand side of Figure 7.3 recent results on a negative-parity band in ^{73}Kr obtained from both EUROBALL [193] and GAMMASPHERE [194] data are compared to the course of the alignment of the even-even nuclei ^{72}Kr [189-191] and ^{74}Kr [195]. Clearly, the crossing frequency for ^{72}Kr ($\hbar\omega \sim 0.9$ MeV) found in these experiments is different from the one observed for ^{73,74}Kr ($\hbar\omega \sim 0.6$ MeV). However, more recent results in ^{72}Kr indicate that the delay in alignment is less pronounced [196]. In all three cases the spin amount associated with the alignment indicates a simultaneous neutron and proton $g_{9/2}$ alignment. On the right hand side of Figure 7.3 the kinematic moments of inertia of several light Se isotopes are plotted. Recent results on the $N = Z + 1$ isotope ^{69}Se [197,198] are compared to heavier even-even Se isotopes (thin dashed lines) and the $N = Z$ nucleus ^{68}Se, in which coexisting bands of oblate and prolate shape have been identified [199]. The positive-parity yrast band of the rather complex and irregular excitation scheme of ^{69}Se is a nice example of prolate-oblate shape coexistence. If one accounts for the polarisation effect of the odd neutron, the moment of inertia of this sequence (grey solid line) seems to evolve from an oblate shape in the beginning to a prolate shape after the first band crossing and possibly back to oblate shape at high spin again.

The advent of the latest generation of 4π Ge-detector arrays has not only enabled the identification of a few excited states of rare isotopes far from stability, it has also enabled us to observe somewhat less exotic nuclear species up to very high angular momenta, and in particular the termination of rotational bands, i.e., the evolution of a given configuration from collective rotation towards a state of single-particle character, for which the individual

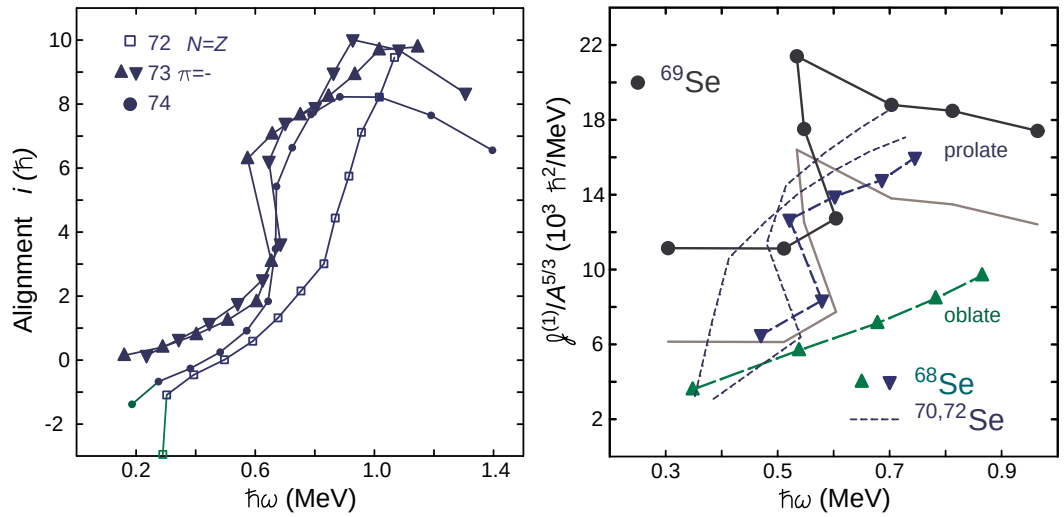

Figure 7.3: *On the left hand side the alignment,* i, *of the positive-parity yrast band in the N = Z = 36 nucleus ^{72}Kr [189,190,191] is compared to the negative-parity bands in ^{73}Kr [193,194] and the positive parity sequence in the even-even neighbour ^{74}Kr [195]. On the right hand side the moments of inertia,* $J^{(1)}$, *of the positive-parity yrast sequence in ^{69}Se [197,198] are compared to neighbouring even-even isotopes, especially to the presumed oblate and prolate bands in the* N = Z *nucleus ^{68}Se [199].*

angular momenta of the participating nucleons are fully aligned along one axis (cf. Section 5). Based on EUROBALL data it was possible to derive the first case of band termination in the A ~ 70 - 80 region, namely in ^{73}Br [141]. The highest states observed lie at about twice the excitation energy (E_{max} ~ 25 MeV) than known from spectrometers of the previous generation, the spin exceeds 30$\hbar$, and the γ-ray energies at the top of the bands (up to E_γ ~ 3.7 MeV) mark the fastest rotating systems ever observed, along with the superdeformed bands in the A ~ 60 region (see above).

The second topic related to high-spin phenomena is the observation of a signature inversion in a pair of negative-parity bands in ^{72}Br [200]. The signature splitting and eventual inversion can best be seen when the energy differences of subsequent states are plotted as a function of spin (see Figure 7.4). In both experiment (top) and calculation (bottom) the signature α = +1 odd-spin states are favoured energetically at low spin, while the inversion occurs at spin I = 16$\hbar$. This is very different from other odd-odd nuclei in the mass region, which often reveal signature inversions in positive-parity bands at relatively low spin I = 9$\hbar$, which is the maximum value of an aligned neutron and proton moving in orbitals of the $g_{9/2}$ shell.

In general, signature inversion is viewed as a fingerprint for triaxiality in nuclei [cf. Section 2]. The only explanation of the high-spin signature inversion in ^{72}Br is the evolution from a triaxial shape rotating around the intermediate axis to a triaxial shape with rotation around the smallest axis [200]. The detailed interpretation of the data reveals the importance of the low-j orbitals of the *fp* shell.

Another significant part of the studies with EUROBALL has been devoted to odd-odd N = Z nuclei. Two issues seem to be important for all such nuclei - the features of rotational bands, which evolve at high angular momentum, and the determination of the T = 1 isobaric analog states, which are difficult to access due to their energetic location relatively high above the

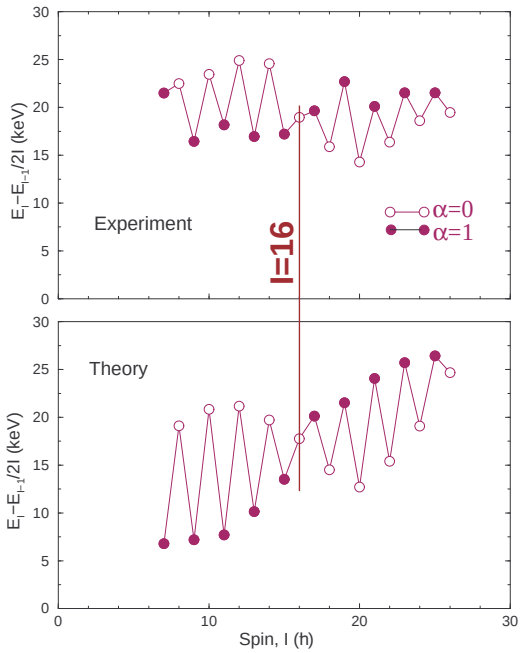

Figure 7.4: *Normalized energy differences between states having spin* I *and spin* I - *1 for the observed (a) and predicted (b) negative-parity band in ^{72}Br [200].*

yrast line. For the former, new results in ^{66}As indicate the existence of a prolate deformed band in the spin regime ~ 13 ≤ I ≤ ~ 23. Interestingly, this band has an unsually large moment of inertia. The analysis is still in progress [201]. Excited states in ^{70}Br were identified for the first time, including T = 1 isobaric analog states up to spin I = 8 [202]. The surprising result is that the energy differences E_x(^{70}Br)-E_x(^{70}Se) take negative values for the four known states, while corresponding numbers for other pairs of nuclei (^{50}Mn-^{50}Cr, ..., ^{74}Rb-^{74}Kr) are basically all positive. In principle one would expect no difference between neutron-proton and neutron-neutron interactions if the states were pure seniority ν = 2 excitations. A positive energy difference implies that more proton pairs have to be aligned in the even-even T_z = 1 nucleus compared to its T_z = 0 odd-odd N = Z neighbour. This can be understood because protons may be bound in neutron-proton pairs in these nuclei. The negative energy difference for the A = 70 pair is probably due its close proximinity to the proton dripline: An increased proton radius due to weak binding leads (*i*) to a reduction of the Coulomb repulsion (Thomas-Ehrman shift) and (*ii*) reduces neutron-proton two-body matrix-elements of in particular low-j orbitals, thus leading to a less bound 0^+ state [202].

7.4. Approaching ^{100}Sn

^{100}Sn is the heaviest particle-bound nucleus having the same number of neutrons and protons, N = Z = 50. It is expected to reveal all the expected characteristics of a doubly magic nucleus lying far from the line of stability. Since doubly magic nuclei can be considered as bench marks within the chart of nuclides, this explains the experimental and theoretical efforts put into the study of nuclei in the vicinity of ^{100}Sn.

A number of experiments at EUROBALL have been devoted to specific aspects of the ^{100}Sn region, namely to study the shell structure by means of investigations of single-particle

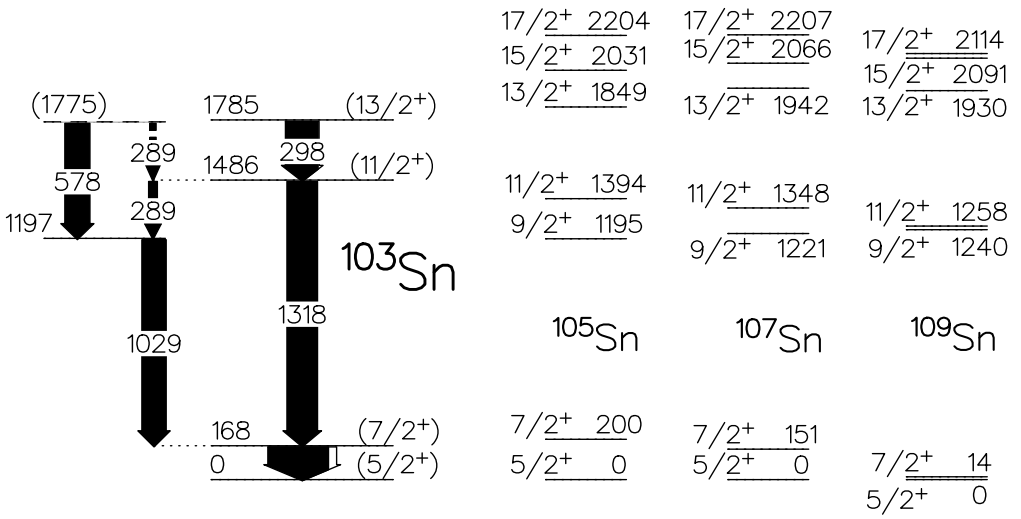

Figure 7.5: *Level scheme of ^{103}Sn [203] and the systematics of odd-*A *neutron-deficient Sn isotopes.*

energies and the two-body (neutron-proton) residual interactions, and core polarizations of various kinds. Of course, the neutron single-particle energies could be derived best from excited states in ^{101}Sn. However, at present this extremely neutron deficient nucleus does not seem accessible for in-beam studies. Therefore, the single-particle energies have to be estimated from known excited states in more remote neighbours of ^{101}Sn by comparing them to predictions of shell-model calculations using an appropriately comprehensive model space as well as a realistic interaction. However, the further away one moves from the doubly magic core the more hampered such estimates become because of uncertain two-body interactions and/or restrictions in the tractable model space.

Currently, the best possible information on neutron single-particle energies comes from new information in ^{103}Sn [203]. Together with ^{97}Ag, which was the focus of another EUROBALL experiment, ^{103}Sn marks the closest approach to ^{100}Sn in terms of odd-A nuclei, the knowledge of which is vital for the experimental determination of the single-particle energies. These in turn provide stringent test of the mean-field models. Figure 7.5 shows on the left hand side the previously unknown excitation scheme of ^{103}Sn, which is compared to heavier odd-A Sn isotopes on the right hand side. The energy difference of 168 keV between the $5/2^+$ and $7/2^+$ states yields the most accurate result to date for the relative energies of the neutron $d_{5/2}$ and $g_{7/2}$ orbitals with respect to ^{100}Sn. Using an interaction based on the Bonn-A potential an energy difference of 110(40) keV can be derived. The error reflects uncertainties related to variations of the effective interaction [203].

The identification of excited states in ^{103}Sn shows that scarce data in exotic nuclei is often more valuable than ample information on nuclei closer to the line of stability. Evidence for excited states in ^{95}Ag has been presented recently [204]. Another key isotope is ^{100}In, which has one neutron and one proton hole relative to the ^{100}Sn core. The identification of excited states in ^{100}In will provide important information on neutron-proton two-body matrix elements. An experiment has recently been performed at EUROBALL to achieve this goal. Presently, excited states in ^{98}Ag, ^{102}In, and ^{106}Sb provide the best grounds for studying the neutron-proton interaction near ^{100}Sn. In particular, resent results in ^{102}In, which include core-excited states, reveal new information on neutron-proton matrix elements, namely on the $\nu(h_{11/2})\otimes\pi(g_{9/2})^{-1}$ multiplet [205,206].

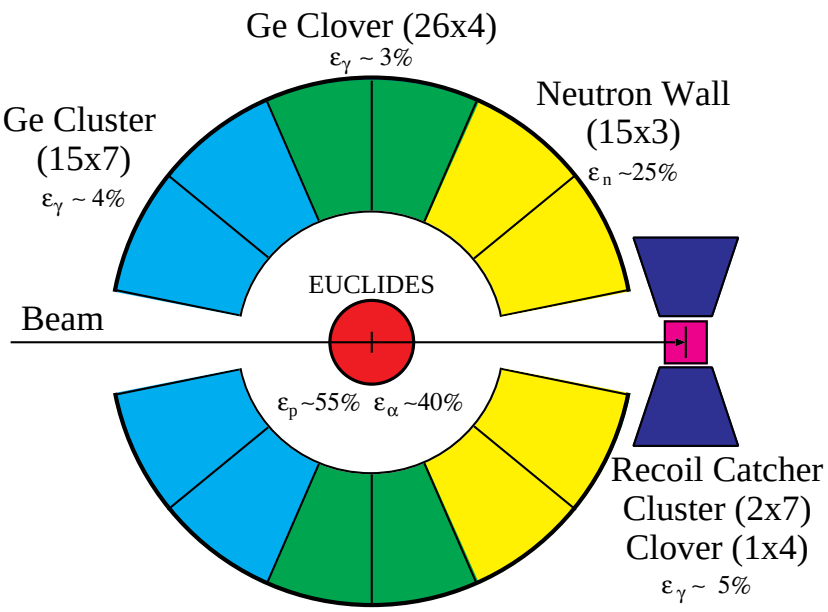

Figure 7.6: *Schematic drawing of the set-up for isomer tagging at IReS, Strasbourg, during the Neutron Wall campaign in 2001.*

The knowledge of excited states in the two T_z = 1 nuclei ^{98}Cd [207] and ^{102}Sn [208] yields the closest approach to ^{100}Sn to date. In both even-even neighbours, μs-isomers have been observed in a series of pre-EUROBALL experiments (PEX) at the NBI Tandem Accelerator Laboratory. The isomeric states correspond to fully aligned $\pi(g_{9/2})^{-2}_8$ and $\nu(g_{7/2})^2_6$ or $[\nu(g_{7/2})\otimes\nu(d_{5/2})]_6$ configurations, respectively. The comparison between the predicted and measured $B(E2;6^+\rightarrow4^+)$ transition strength in ^{102}Sn yields a relatively large polarizability induced by the two extra neutrons. However, the derived effective neutron charge, e_ν ~ 2.0, is model dependent, because the wave functions of both the initial and final state, which are mixtures of mainly $d_{5/2}$ and $g_{7/2}$ components, rather strongly depend on the shell-model parameters used. In turn, the wave function of the 8^+ state in ^{98}Cd turns out to be rather insensitive to the parametrisations, while the originally measured half-life of the 8^+ isomer calls for an unexpectedly low effective proton charge of e_π ~ 0.9 [207].

The presence of a second, higher-lying isomer would be a possible solution to increase the effective proton charge to values in excess of unity. Indeed, an isomer study of neutron deficient nuclei near ^{100}Sn using a fragmentation reaction and subsequent in-flight separation techniques reported a shorter half-life for the 8^+ state in ^{98}Cd, which can be attributed to the on average lower angular momentum input of fragmentation reactions, i.e., the second, higher-lying isomer has not been populated.

The similarities between the shell structure of the ^{56}Ni and ^{100}Sn regions shall not remain unmentioned (see, e.g., Ref. [209] for a recent review). For example, polarisation effects or $E2$ and $M1$ correlations across the double shell closure should be present in both cases. In this respect it is interesting to note that (*i*) there is a well-known 10^+ high-spin isomer in ^{54}Fe, which is the two proton-hole nucleus relative to ^{56}Ni, and (*ii*) that the 2668 keV $6^+\rightarrow4^+$ core excitation transition in ^{58}Ni is nearly identical to the 2701 keV 2^+ energy in ^{56}Ni. Therefore, the identification of the corresponding core excited states in the ^{100}Sn region was the focus of two recent EUROBALL experiments aiming at ^{98}Cd and ^{102}Sn. Their dedicated set-up is

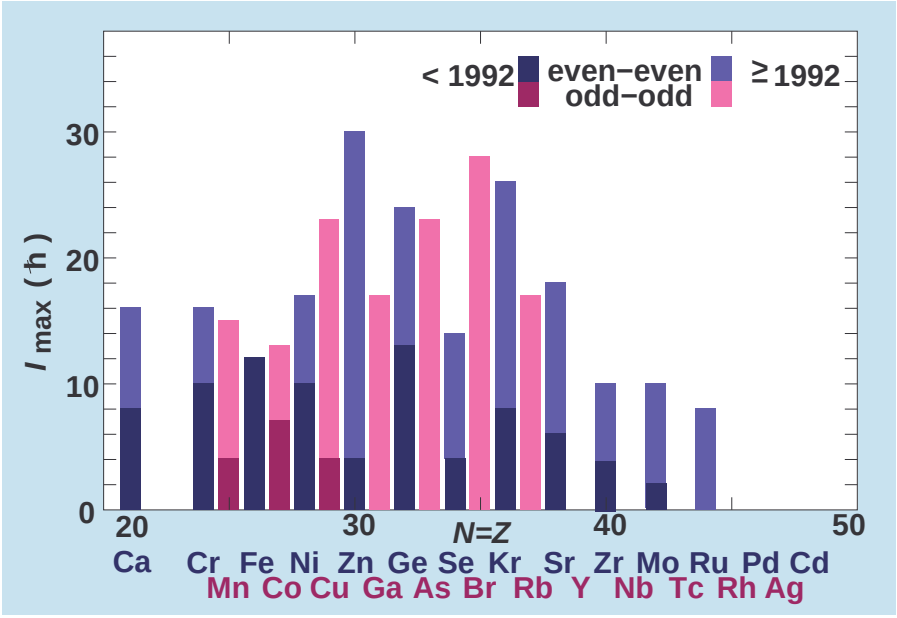

Figure 7.7: *Maximum spin values, I_{max}, reached for discrete in-beam γ-ray spectroscopy of $N = Z$ nuclei between Ca and Sn as of summer 2002.*

sketched in Figure 7.6 and is a close resemblance of the original set-up used at NBI: The prompt evaporated particles are detected in EUCLIDES [5] and the Neutron Wall [7] and correlated with delayed γ-rays detected in two Cluster and one Clover Ge detector surrounding the recoil catcher. The combined information of these detector systems is then used to tag prompt γ radiation measured with the standard Cluster and Clover sections of EUROBALL. The analysis of these two experiments is in progress.

7.5. Perspectives

The combination of powerful ancillary devices and the EUROBALL spectrometer has led to a significant increase in knowledge concerning $N \sim Z$ nuclei over the past few years. This is summarized schematically in Figure 7.7, which provides the maximum spin values reached for discrete in-beam γ-ray spectroscopy of $N = Z$ nuclei before (dark histograms) and after 1992 (light histograms), i.e., with the advent of the latest generation of 4π Ge-detector arrays.

The limit of spectroscopy has been pushed into the Zr region, while the observation of a few states up to ^{96}Cd appears feasible with present day technology and techniques. The study of excited states in odd-odd $N = Z$ nuclei seems to be limited to ^{78}Y, because starting from ^{82}Nb their production via stable beam-target combination involves the evaporation of at least three neutrons. Thus the next major breakthrough, for example, the identification of the 2^+ state in ^{100}Sn, will have to wait for the currently projected 4π gamma-tracking arrays (AGATA and GRETA), improved ancillary detectors, and possibly involve the use of (re-accelerated) unstable ions.

Until then, further evidence for the influence of neutron-proton pair correlations on high-spin properties might be gathered from either very high spin states in e.g., ^{48}Cr, or by deducing more detailed spectroscopic information for the heavier even-even $N = Z$ systems such as

^{72}Kr, ^{74}Rb, ^{76}Sr, or possibly ^{80}Zr via lifetime measurements. Similarly, the quest for excited states in rare isotopes will continue - experiments have been performed at EUROBALL to hunt for ^{78}Y, ^{96}Cd, and ^{100}In.

Another direction could be more elaborate studies of particle-γ correlations, including the evaporated (charged) particles from the compound systems. Eventually hyperdeformed structures at very high angular momentum in more strongly populated nuclei near the $N \sim Z$ line may become tractable.

Finally, other in-beam techniques are going to be exploited in the near future. For example, there are going to be attempts to further tighten the limits of the shell model parameters around ^{100}Sn by measuring the $B(E2;2^+ \rightarrow 0^+)$ values for several $N = 50$ isotones and light Sn isotopes via relativistic Coulomb excitation of secondary beams in the framework of the RISING campaign at GSI Darmstadt employing EUROBALL Cluster detectors. Further, new or updated techniques with respect to these fast radioactive secondary beams are currently being considered to derive static electric or magnetic moments of specific states or structures along the $N = Z$ line.

Acknowledgements

The author is very grateful to G. de Angelis, C. Fahlander, M. Górska, T. Martinez, J. Nyberg, C. Plettner, D. Sohler, I. Stefanescu, and T. Steinhardt for fruitful discussions and/or for allowing me to use their material in this contribution.